Hanke, S.; Beyer, M.; Silvonen, A.; dos Santos, J.F.; Fischer, A.:

Cavitation erosion of Cr60Ni40 coatings generated by friction surfacing

In: Wear (2012) Elsevier

DOI: 10.1016/j.wear.2012.11.016

Cavitation Erosion of Cr60Ni40 Coatings Generated by Friction Surfacing

S. Hanke[*1], M. Beyer[2], Aulis Silvonen[3], J. F. dos Santos[2], A. Fischer[1]
[1]*University of Duisburg-Essen, Materials Science and Engineering, Lotharstr.1, Duisburg, Germany*
[2]*Helmholtz Zentrum Geesthacht, Institute of Materials Research, Max-Planck-Straße 1 , Geesthacht, Germany*
[3]*Wärtsilä Finland Oy, Vaasa, Finland*

Received Date Line (to be inserted by Production) (8 pt)

Abstract

CrNi-alloys with high Cr-content generally are quite brittle and, therefore, only available as castings and regarded as neither weldable nor deformable. The process of friction surfacing offers a possibility to generate Cr60Ni40 coatings e.g. on steel or Ni-base substrates. Cavitation tests were carried out using an ultrasonic vibratory test rig (~ASTM G32) with cast specimens and friction surfaced coatings. The coatings show less deformation and smaller disruptions, and wear rates in steady state were found to be three times higher for the cast and heat treated samples than for the coatings, caused by a highly wear resistant Cr-rich phase. The results of this study show that it is possible to generate defect free coatings of Cr60Ni40 with a thickness of about 250 µm by friction surfacing, which under cavitation show a better wear behavior than the cast material. Thus, in combination with a ductile substrate, these coatings are likely to extend the range of applicability of such high-temperature corrosion resistant alloys.

Keywords: solid-state joining, hardfacing, two-phase alloy, microstructure

1. Introduction

The alloys of Cr60Ni40-type (ASTM A560) inhibit an outstanding high-temperature corrosion resistance and, therefore, were applied in the past for refinery furnaces [1] and applications with comparable operational demands. They have a high strength, but are quite brittle due to the high Cr-content. Values required by the ASTM standard [2] for mechanical properties and chemical composition are given in Table 1. Cr60Ni40 is regarded to be non-deformable and non-weldable, therefore being only available as castings.

*Corresponding author. Tel.: +49 203 379 1298; fax: +49 203 379 4374.
E-mail address: stefanie.hanke@uni-due.de (Stefanie Hanke)

Table 1. Chemical composition and properties of Cr60Ni40 according to ASTM 560/A 560 M [2]

C	Mn	Si	S	P	N	Fe	Ti	Al	Cr	Ni
< 0.1	< 1.0	< 1.0	< 0.2	< 0.2	< 0.3	< 1.0	< 0.5	< 0.25	58.0 - 60.0	balance
tensile strength > 760 MPa						yield strength > 590 MPa				

A second large field of applications for Cr-Ni alloys is as thin film resistors in microelectronics. For this reason, the structure and electrical properties of alloys with various Cr-Ni-ratios have been extensively studied in thin sputtered films, leading to the identification of several non-equilibrium phases [3-6].

For the binary Chromium-Nickel system, usually three equilibrium solid state phases are denoted, being each fcc Ni- and bcc Cr-rich solid solutions as well as an ordered Ni_2Cr intermetallic phase below 590°C [3, 7]. A eutectic exists which is reported by different authors ranging from 46 to 49 wt-% Ni and 1327 to 1345°C [1, 7, 8]. A calculated phase diagram from [9] is presented in Fig. 1. Additionally, several non-equilibrium phases are reported, most frequently identified as tetragonal σ phase or cubic δ phase. One reason for the multitude and the partly non-conclusive discussion of phases in Cr-rich Cr-Ni-alloys is the low solubility of Ni in Cr at room temperature. While at the eutectic temperature approximately 35 wt-% Ni can be dissolved, this value drops rapidly with temperature, so that below 900°C less than 5 wt-% are solvable, with a further decrease down to room temperature. Exact numbers for the solubility of Ni in Cr at room temperature are not given [3-7].

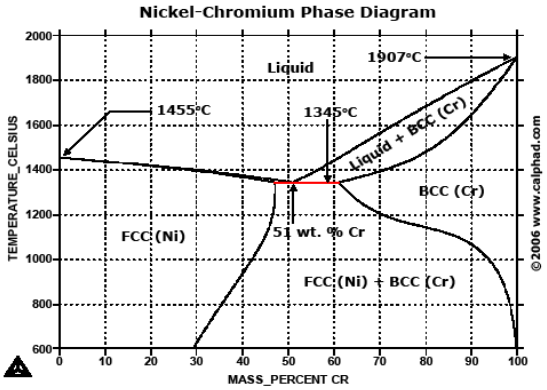

Fig. 1. Phase diagram of Cr-Ni system [9].

Friction surfacing is a solid state joining process, which is accomplished by pressing a rotating rod, made from the coating material, onto a substrate. The rod tip is plasticized by the frictional heat and shear forces and when a translational movement is superimposed, the plasticized material is transferred onto the substrate. Due to the severe plastic shear deformation and high cooling rate the coatings remain in a wrought and quenched state with a microstructure being finer and more homogenous than that of the casting. Details of the process have been published amongst others in [10-12].

This contribution shows that it is possible to generate Cr60Ni40 coatings on Nimonic 80A substrate. The evolution of the microstructure and hardness are discussed. In order to investigate one aspect of the wear behavior, cavitation tests were carried out using an ultrasonic vibratory test rig (~ ASTM G32), comparing the original as cast state and the friction surfaced coatings. The presented results indicate that these Cr60Ni40 coatings, in combination with a ductile substrate, are likely to extend the range of applicability of this high-temperature corrosion resistant alloy.

2. Experimental Methods

2.1 Friction Surfacing of Cr60Ni40

For the coating process, sheets from Nimonic 80A alloy (ASTM B 637; 2.4631) with a thickness of 10 mm were used as substrate material. This high-temperature alloy contains about 70 wt-% of Ni, 20 wt-% Cr and some small additions of Ti, Al and Fe. The surface of the sheets was ground plane, and was prepared for the surfacing process by degreasing with acetone.

The rods from Cr60Ni40 had a diameter of 20 mm. Single and multiple overlapping coatings were prepared, with a rotational speed of the rods of 3500 min^{-1}. At the beginning of the process, the rotating rod was pressed onto the substrate with a downforce of 28 kN and kept for 110 s. In this period, the substrate was warmed by the frictional heat and the material in the rod tip was sufficiently plasticized. The latter was assessed by measuring the shortening of the rod under the applied pressure, which was 3 mm in the preheating phase. The translational movement was then applied with a speed of 0.33 m/min. In friction surfacing not the complete amount of plasticized rod material is transferred onto the substrate, but some portion is pushed up around the rod to build up a flash. If this flash cannot be removed during surfacing and reaches the clamping of the rod the process must be stopped. A detail of the ongoing process is presented in Fig. 2 (a). Wider coatings were produced by overlapping several layers with an offset of 10 mm. Fig. 2 (b) and (c) show a single and a triple-layer coating respectively.

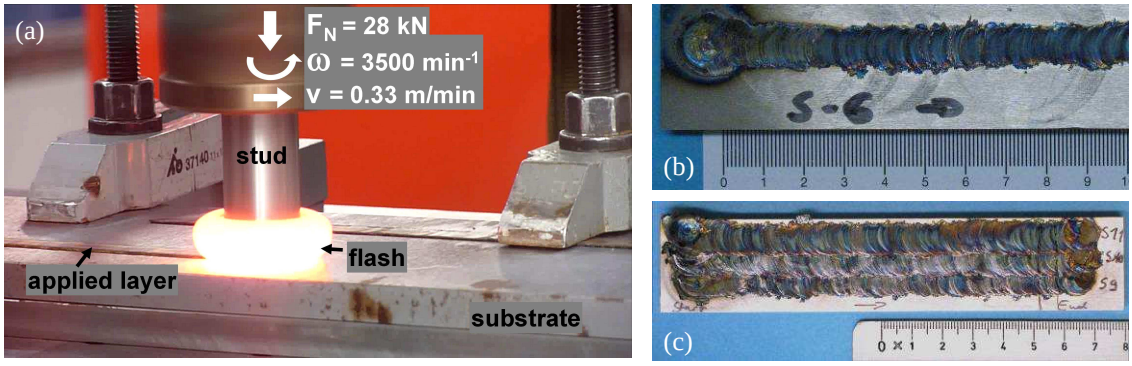

Fig. 2. (a) Detail of the friction surfacing process of Cr60Ni40, (b) single and (c) triple-layer coating.

2.2 Metallographic methods

The rods used to produce the coatings by friction surfacing were machined from commercially available cast and heat treated components. Cross sections were prepared by standard metallographic methods from such material and examined by light- (BX41TF, Olympus Optical Co. Ltd., Tokyo, Japan) and scanning-electron-microscopy (Leo 1530 Gemini, Carl Zeiss Microscopy GmbH, Jena, Germany) including energy dispersive X-ray analysis (EDX) (Apollo X10, EDAX Inc., Mahwah, USA). To reveal the microstructure the polished samples were etched with a solution containing 100 ml HCl, 100 ml H_2O, 10 ml HNO_3 and 1 ml Dr. Vogels' etchant (Buehler GmbH, Düsseldorf, Germany), which contains propanol and thiourea. Cross sections of the single and overlapping coatings were prepared with the visible plane perpendicular to the welding direction by means of the same method.

For further analyses of the microstructural changes of Cr60Ni40 during friction surfacing, samples were prepared from the coatings for transmission-electron-microscopy (TEM). For this purpose, sections of coating layers were cut off the substrate and ground to foils of 100 µm thickness on SiC grinding paper. Discs of 3 mm diameter were punched from the foils and further thinned by electrochemical jet polishing (TenuPol-3) using A2 electrolyte (Struers GmbH, Willich, Germany). A Phillips EM 400 microscope with an accelerating voltage of 120 kV was used for the investigations (Philips Electronics Nederland B.V., Eindhoven, Netherlands).

2.3 Cavitation testing

Samples for cavitation testing were prepared from cast and heat treated material as well as triple-layer Cr60Ni40 coatings. They were cut to sizes of about 25 x 25 mm, and 10 mm thickness. All samples were ground to be plane and then polished with diamond suspensions down to a grain size of 3 µm.

The cavitation testing was carried out following ASTM G 32-03 [13] with some modifications. In the set up a sample was fixed in a rigid holder and immersed into distilled water to a depth of 12 to 15 mm below water level. A double walled container was used in order to keep the water temperature at 25 ± 3 °C by a cryostat (Haake K20, Fisons Instruments GmbH, Karlsruhe, Germany) throughout each experiment. An ultrasonic generator was used to excite a sonotrode to oscillate at 20 kHz with an amplitude of 19 µm during the experiments. The exchangeable flat tip of the sonotrode had a diameter of 16 mm and was positioned 0.5 mm above the sample. The fast oscillation of the sonotrode induces cavitation in the gap between the sample surface and the sonotrode tip. In this set-up, the sonotrode tip is exposed to the same loading as the sample, and therefore also experiences wear. The tips used in the present study are made from the cold hardening stainless steel X13CrMnMoN18-14-3 (1.4452, "P2000") and were replaced and refurbished after 6h of cavitation testing. Each experiment was run in certain intervals, after which the sample was removed from the test rig, cleaned with acetone in an ultrasonic cleaning bath, thoroughly dried and then weighed. Each weight measurement was repeated 5 times on a scale with a

precision of 10^{-4} g (AC211S, Sartorius AG, Goettingen, Germany). Additionally, the wear appearances were investigated by scanning-electron-microscopy (SEM). Three samples of each state were tested.

3. Results

3.1 Microstructure of cast and heat treated state

Before friction surfacing the microstructure in the rods shows the dendritic structure being characteristic for the cast state (Fig. 3 (a)). The darker regions are rich in Cr, while the regions with a brighter appearance show the lamellae of the eutectic solidification (Fig. 3 (b)). Within the Cr-rich regions, a needle-shaped internal structure becomes visible after etching. Here, Ni-rich phases are present as well (Fig. 3 (d)). Presumably these stem from segregation processes during cooling, which can be attributed to the low solubility of Ni in Cr, as mentioned before (Fig. 1). The chemical composition of the different phases was analyzed by EDX attached to the SEM. Within the areas with needle-shaped internal structure the Cr:Ni ratios varied between 57:43 and 61:39 in wt-%. The Ni-rich phases within these areas have a Cr:Ni composition of 48:52. For the eutectic areas the Cr:Ni ratios ranged from 47:53 to 50:50. Spherical non-metallic inclusions rich in Si, Mn, and O are found throughout the samples (blue arrows in Fig. 3 (a and c)).

3.2 Microstructure and hardness of coatings

A light-optical image of the etched cross section through a single layer coating, perpendicular to the welding direction, is presented in Fig. 4. The Nimonic substrate was not affected by the etchant. At both edges along the coating a lack of fusion is visible because the applied downforce is not transformed into a sufficient contact pressure at the outer diameter of the rod. The coating layers have a thickness of 247 ± 41 µm and a gross width of 10.9 ± 0.9 mm, of which 8.7 ± 0.7 mm are bonded to the substrate. These data were obtained from six different single layer coatings, each measured in three positions.

No defects, voids or other peculiar features were found at the bonding line. After etching, darker and brighter regions are visible in the coatings by light microscopy, showing the material flow during the coating process (Fig. 5 (a)). Further grain boundaries are visible in the darker etched areas as well as small precipitates within the brighter one (Fig. 5 (b)). Fine needle-shaped precipitates become visible within the more strongly etched phase (Fig. 6 (a) area 1 and Fig. 6 (b)). Measurements of the local chemical composition of the material were obtained by EDX in the SEM and, with some local variations, average ratios of Cr to Ni in the two main phases were found, as indicated in Fig. 6. In the more strongly etched regions, the average ratio in wt-% of Cr to Ni was found to be 63:37, and in the constituents less affected by etching, it is 52:48. Additionally, approximately 1.2 wt-% of Fe were found in all constituents. Mn, Si and Ti were only found in the spherical non-metallic inclusions, which are still present as seen in the cast and heat treated state.

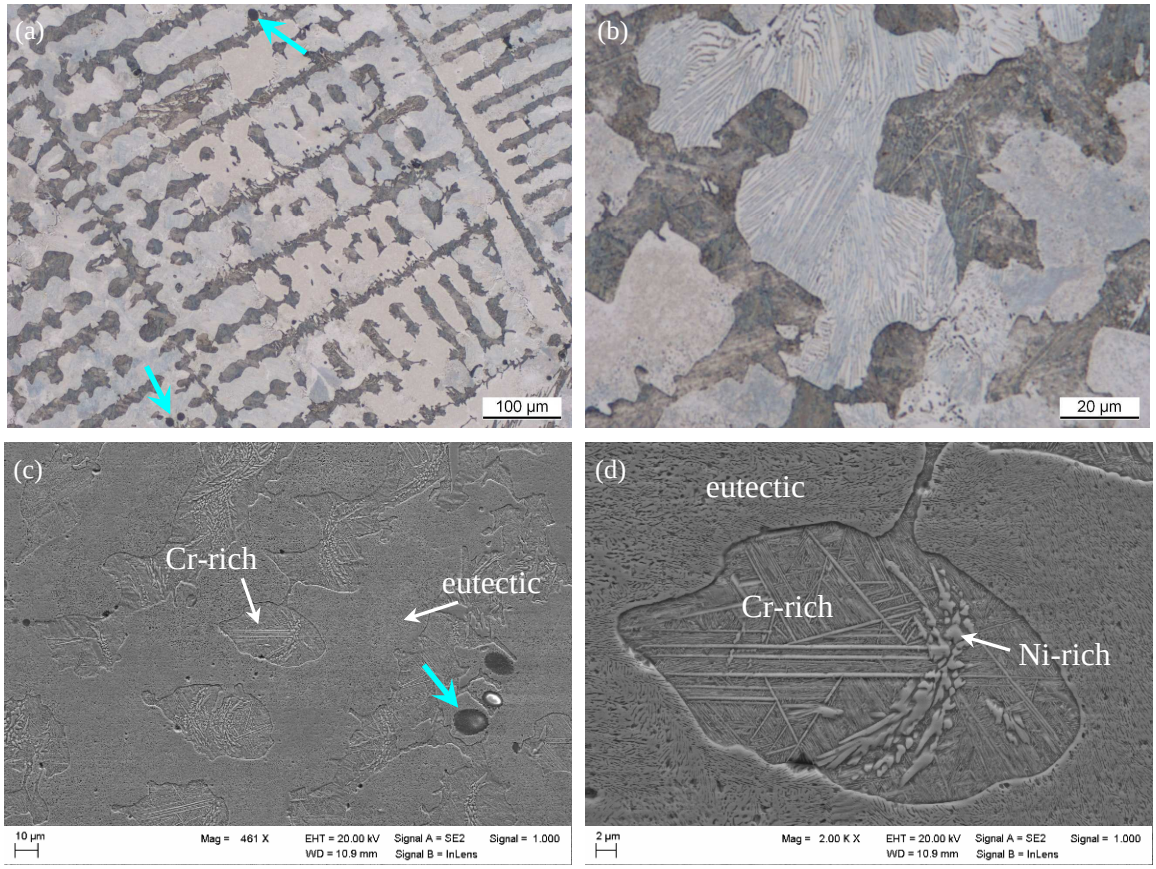

Fig. 3. Microstructure of the cast and heat treated state of Cr60Ni40. The brighter regions are the eutectic phase, the darker ones are a Cr-rich phase containing additionally Ni-rich precipitates. The blue arrows denote non-metallic inclusions rich in Mn, Si and O.

Fig. 4. Cross section of a single layer coating.

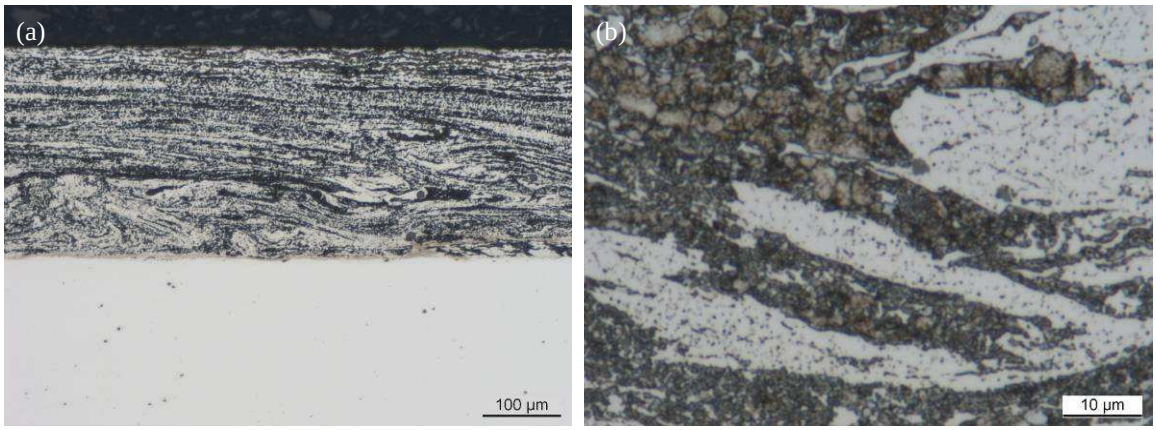

Fig. 5. Cross section of a Cr60Ni40 coating, showing (a) complete coating thickness as well as part of the substrate, and (b) two-phase microstructure with small precipitates.

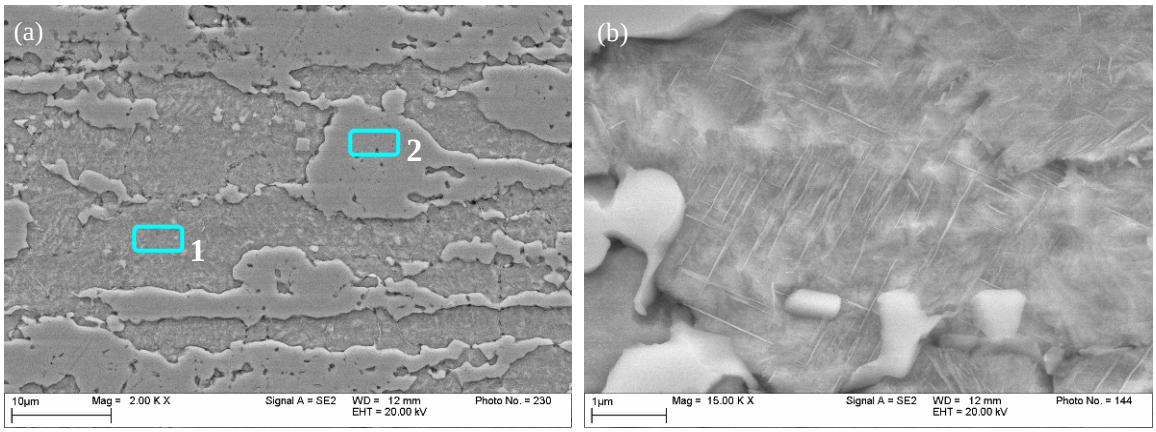

Fig. 6. Cross section of a Cr60Ni40 coating (etched), showing the two-phase microstructure and the fine needle-shaped precipitates within the more strongly etched phase. The average ratios of Cr:Ni determined by EDX in several measurements are 63:37 and 52:48 within the exemplary areas 1 and 2, respectively.

Hardness measurements were conducted on single layer cross sections by the Vickers' method using a weight of 5 kg (HV0.5). The first measurements were placed 50 µm below the coating surface and the following ones were placed at distances of 100 or 200 µm advancing into the substrate material. In Fig. 7 measurements in the centre of three different coatings are presented. The hardness is highest within the coatings and ranges from 420 to 550 HV0.5. Underneath the coatings, a significant drop in hardness to 270 HV0.5 is found within the heat affected zone, followed by a rise to that of the substrate of about 400 HV0.5.

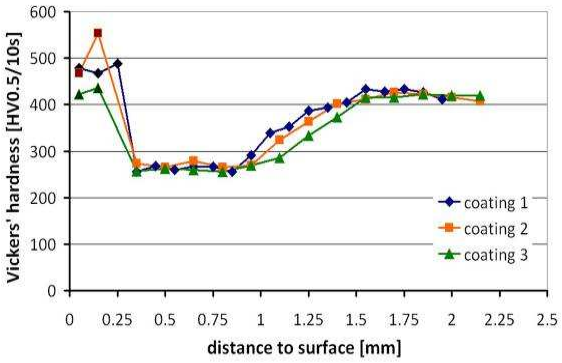

Fig. 7. Hardness profile of single layer coatings starting 50 µm underneath the coating surface.

3.3 Multiple overlapping layers

The multiple overlapping layers show the same microstructural features as the single layers. The lack of fusion could be bonded to the substrate by the heat and pressure from the overlapping layers. The bonding between the layers is free of defects; still occasionally oxide inclusions were found. The overlap regions can be identified within the cross sections by the flow lines of the material depicting the mechanical intermixing (Fig. 8 (a)). Still a lack of fusion cannot be avoided at the edges of the last layer (Fig. 8 (b)).

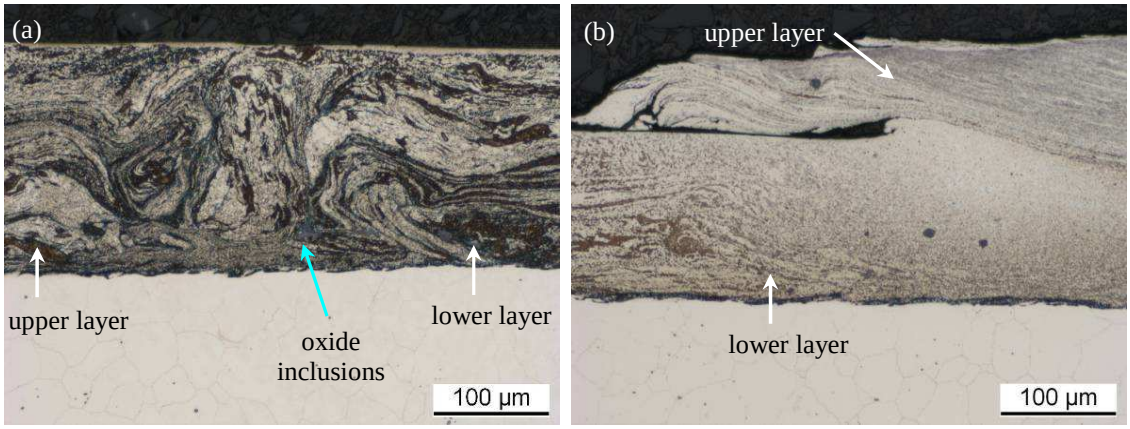

Fig. 8. Cross section of triple-layer Cr60Ni40 coatings (etched), showing the overlap regions between two layers.

3.4 Wear progression under cavitation

In Fig. 9 to Fig. 15, SEM pictures of samples' surfaces after different intervals of cavitation testing are presented in parallel in order to demonstrate the major differences of the wear appearances. After 45 min the cast and heat treated samples show outlines of grains and non-metallic inclusions have been pulled out (Fig. 9 (a)) while the coatings present only very small voids related to fine oxide particles (Fig. 9 (b)).

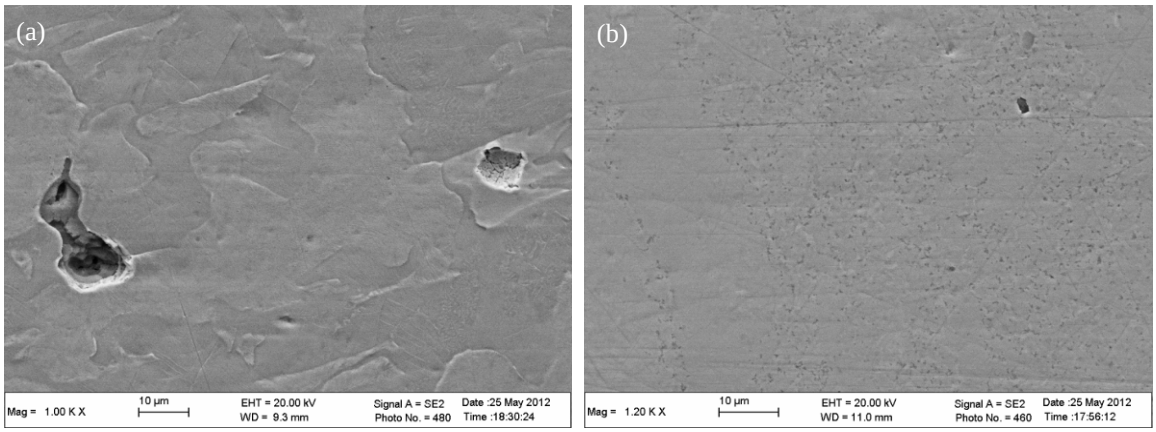

Fig. 9. Surface after 45 min of cavitation, (a) cast and heat treated state and (b) coating.

After 120 min, inter- and transgranular microcracks lead to delaminations of up to about 50 µm in size all over the worn surface of the cast and heat treated samples (Fig. 10 (a), Fig. 11 (a)). In addition plastic deformation can be seen within the eutectic areas (Fig. 11 (b)). For the coatings the two main constituents become slightly distinguishable and few pull-outs are visible (Fig. 10 (b)).

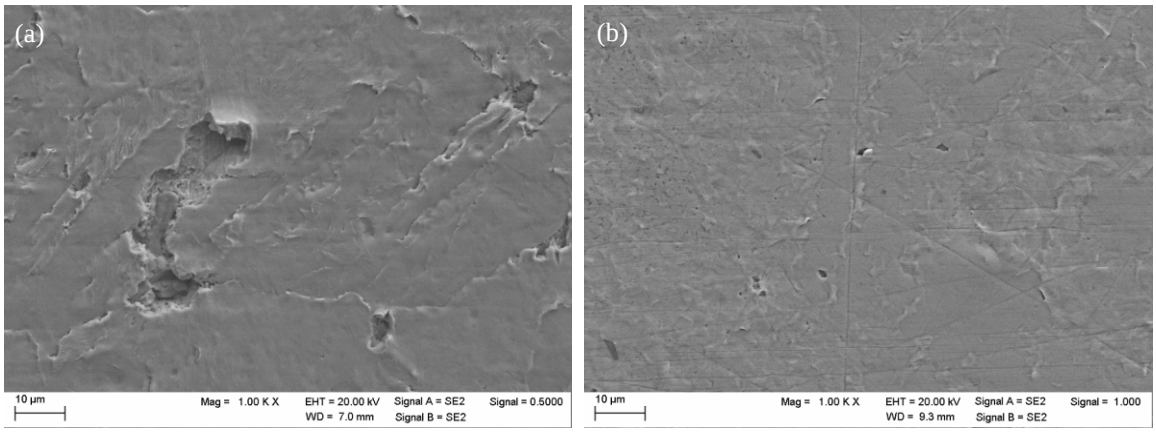

Fig. 10. Surface after 120 min of cavitation, (a) cast and heat treated state and (b) coating.

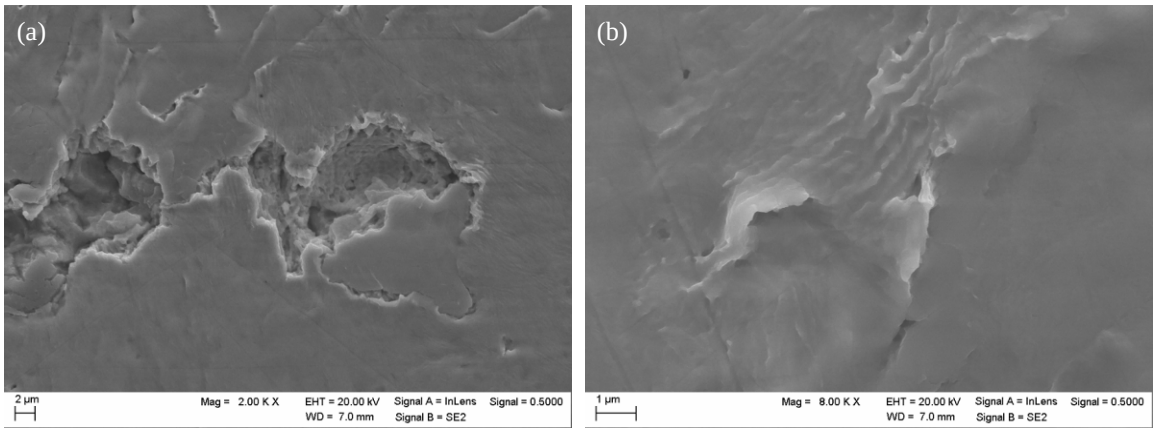

Fig. 11. Surface after 120 min of cavitation on cast and heat treated sample.

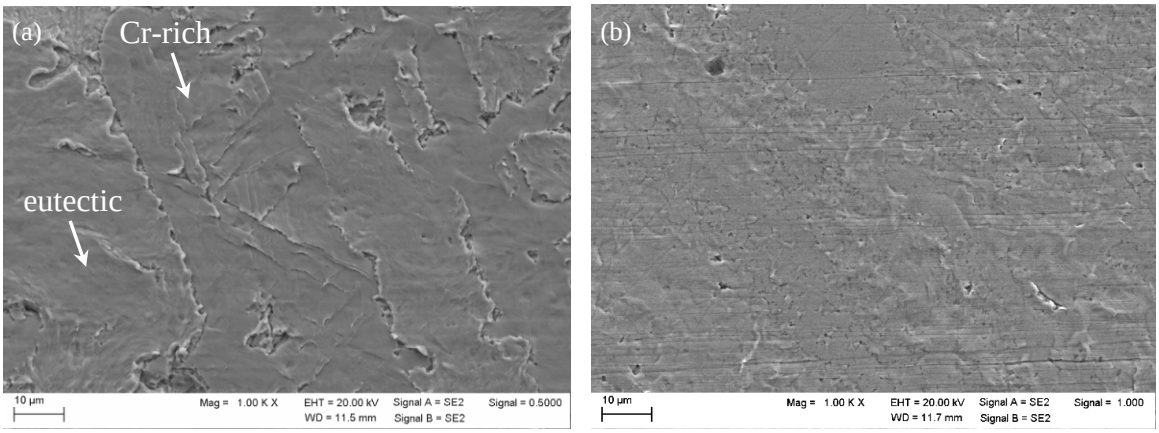

Fig. 12. Surface after 180 min of cavitation, (a) cast and heat treated state and (b) coating.

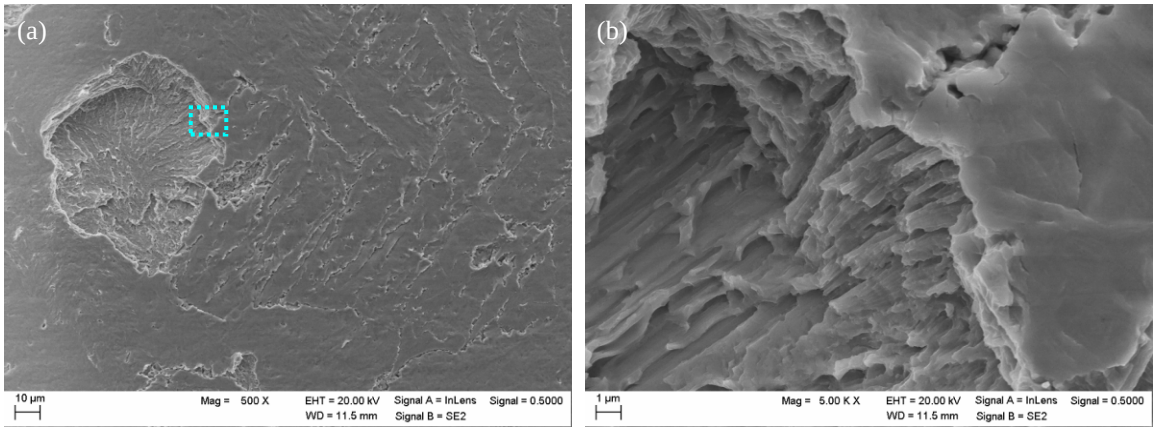

Fig. 13. Surface after 180 min of cavitation on a cast and heat treated sample, (b) showing a detail of (a).

Delamination and plastic deformation proceed with advancing test duration. In the cast and heat treated state, after 180 min cracks no longer prevail at the phase boundaries, but are also visible within the Cr-rich phase

(Fig. 12 (a)). Still material removal is mainly brought about within the eutectic areas (Fig. 13). Again the coatings show less cracks and pull-outs (Fig. 12 (b)).

After 300 min it becomes visible, that for the cast and heat treated samples both main phases, the eutectic and the Cr-rich constituent, have been affected by cavitation. Size and number of delaminations increased significantly (Fig. 14 (a)), while for the coatings it appears predominantly for one phase (Fig. 14 (b)). This tendency persists even after 540 min. While for the cast and heat treated samples, the surfaces wear extensively, for the coatings one phase endures. Even now it still shows polishing marks from sample preparation (Fig. 15). This most resistant phase could be identified by EDX by a Cr:Ni ratio of 63:37 as the Cr-rich constituent with internal needle-shaped precipitates.

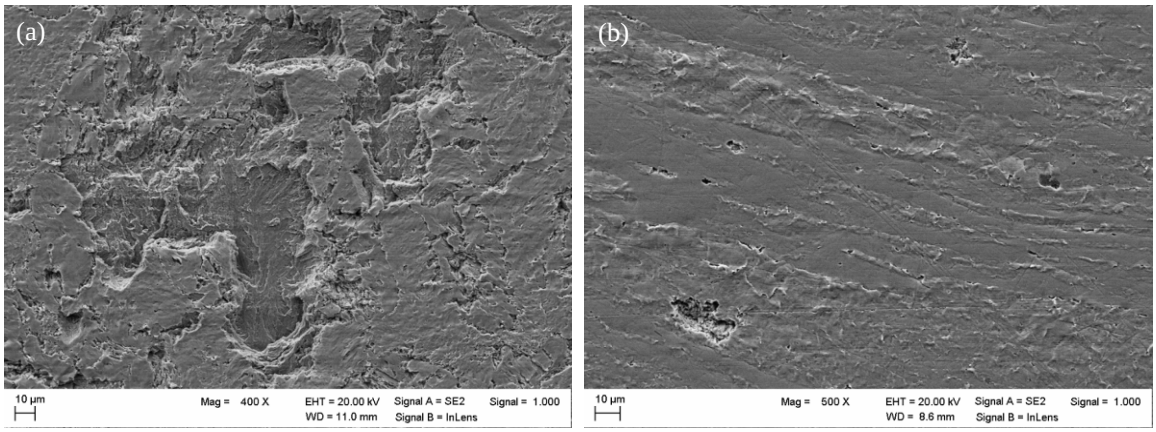

Fig. 14. Surface after 300 min of cavitation, (a) cast and heat treated state and (b) coating.

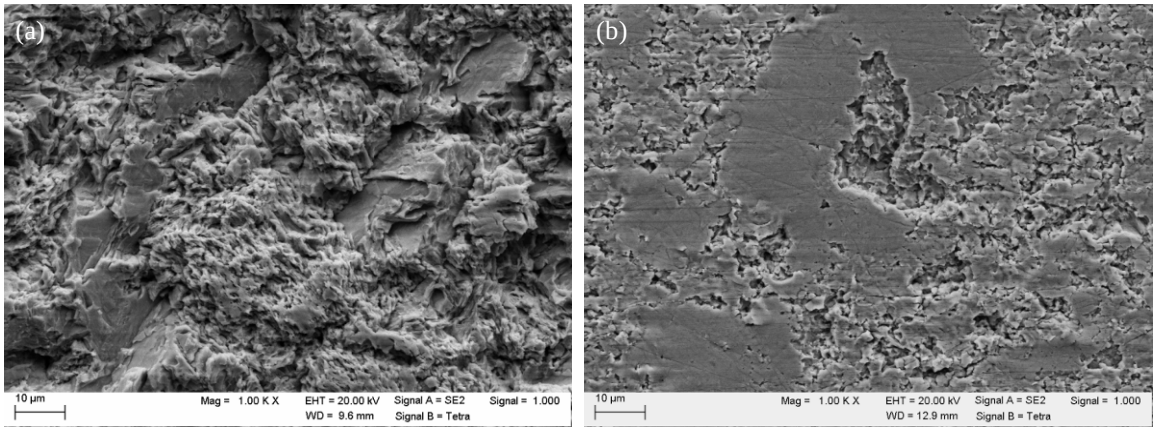

Fig. 15. Surface after 540 min of cavitation, (a) cast and heat treated state and (b) coating.

The weight loss measured in between the intervals of cavitation testing is presented for two exemplary samples in Fig. 16. No incubation time within the first minutes of testing was found, and up to 120 min a steady wear took place, similar for both types of samples. Following this the curves decline with the weight approaching

the original value again. This increase in weight was found on all samples and in a similar range both in magnitude of weight "gain" and time of testing, though slight differences were visible when shorter intervals where chosen for a cavitation test. A possible explanation for this behavior could be that water has entered fine cracks and voids which formed in the first stages of loading, e.g. along phase boundaries (see Fig. 12), leading to an increase in measured weight. It was not possible to eliminate this effect by heating or evacuating the samples before weighing, which might be explained by a capillary attraction of very fine cracks. With continuing cavitation the discontinuities on the surfaces become larger, disabling possible capillarity effects, and therefore leading to a measurable weight loss again (see Fig. 14). Nevertheless, after 360 min of testing it becomes obvious, that the wear rate of the coating is lower than that of the cast and heat treated one. Thus after 420 min the coatings wear by an average of 0.013 mg/min, while the cast and heat treated samples show a higher rate at 0.037 mg/min.

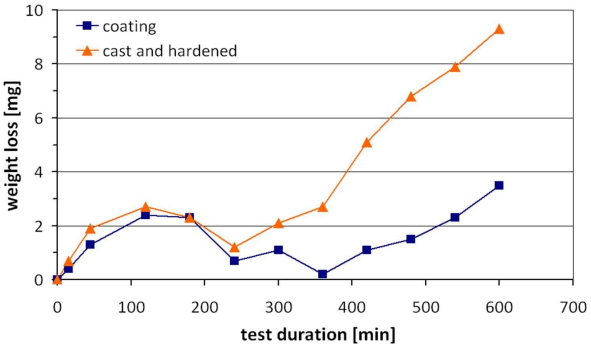

Fig. 16. Progression of weight loss during cavitation for a cast and heat treated and a coating sample.

4. Discussion

4.1 Evolution of the microstructure

As discussed earlier, the microstructure of cast Cr60Ni40 alloys is quite complex despite of the rather simple phase diagram. The dendritic microstructure consists of two areas, which obviously are mixtures of different phases. One exhibits eutectic lamellae and the chemical composition was found to roughly match the eutectic, with a slightly increased Ni content. The second one contains approximately 60 wt-% Cr, which equals roughly the composition of the Cr-rich bcc-crystal just below the eutectic temperature (Fig. 1). The needle-shaped inner structure found in these regions was described in [14] as Ni-rich Widmannstätten precipitates, which form – possibly via an intermediate hexagonal β phase [15] – during cooling with the decrease in Ni-solubility, and are assumed to be embedded in the remaining Cr-rich solid solution phase. The larger, Ni-rich precipitates, which are also found within the Cr-rich regions, seem to have formed earlier than the finer Widmannstätten needles, since they are more bulky in shape (Fig. 3 (d)), and have a composition similar to the one of the eutectic regions. Even though in EDX measurements some process-related deviations in the quantitative results must be expected, it is

clear that the cast material is not in a complete equilibrium state. Since this material was industrially manufactured by centrifugal casting, an economically sensible cooling rate would have been chosen.

During the process of friction surfacing forging temperatures are reached. The color of the glowing flash during the process is light yellow, pointing to temperatures above 1200°C (Fig. 2 (a)). Still, the heat input is low, compared to fusion welding, since the high temperature is localized within the plasticized material layer at the rod tip [16], and rapid cooling by heat flow into the machine bed and the surroundings takes place. At the same time, a high degree of plastic deformation of the plasticized material takes place, promoting dissolution and an even distribution of the alloy's constituents, followed by recrystallization during cooling [17].

As a consequence of such severe plastic deformation followed by quenching, no eutectic lamellae have been found in the coatings, but a phase with the Cr:Ni ratio of the eutectic (52:48), which was not attacked by the etchant (Fig. 5 (b), Fig. 6 (a)). Presumably this is a supersaturated solid solution generated by the solution of the eutectic phases during heating, while quenching avoided reprecipitation. These findings are supported by TEM investigations (Fig. 17). The solid solution shows twins and dislocations, which points to some residual deformation. Diffraction patterns confirm an austenitic fcc structure of the Ni-rich phase (Fig. 17 (a)).

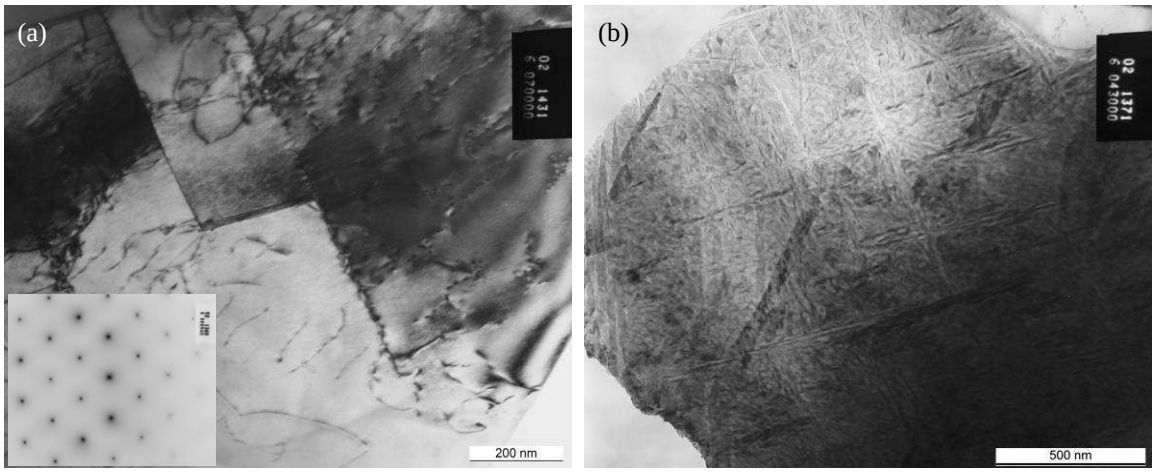

Fig. 17. TEM images of Cr60Ni40 coating, (a) supersaturated solid solution, (b) Cr-rich grain.

The other grains appear similar to the Cr-rich constituent in the cast material with needle-shaped precipitates of Widmannstätten type. From Fig. 3 (d) and Fig 6 (b) it can be seen, that the precipitates are much finer within the coatings, which can be attributed to the severe plastic deformation and high quenching rate. TEM also reveals the high volume fraction of fine precipitates within the Cr-rich constituent (Fig. 17 (b)).

4.2 Influence of the microstructure on wear progression

The damage on the surfaces of the cast and heat treated samples clearly starts at the phase boundaries. This is a mechanism found regularly on surfaces exposed to cavitation, and is due to the mechanical impact stresses caused by imploding cavitation bubbles. If two adjacent grains or phases have different strength and ductility, the strain will be larger in the weaker phase, leading to stresses within the boundary [12, 18]. Within the eutectic the fcc NiCr solid solution obviously is the weaker phase and protrudes in between the harder CrNi lamellae. The Cr-rich constituent starts to show microcracks after about 180 min while all constituents are wearing at the end of the experiments at 600 min.

For the coatings the same mechanisms and sequence are found but to a much smaller extent and in a larger period of time. The supersaturated austenitic solid solution is the phase being worn first, but in the beginning it merely shows deformation or roughening. Remarkable delaminations are found after about 300 min. Again the Cr-rich constituents last longer and occasional cracks can be found only after 600 min. Most of these areas still show no marked appearances of cavitation.

In conclusion both main constituents perform better within the coatings. Wear proceeds faster for the cast and heat treated samples by deformations within the eutectic grains, leading to large delaminations. Even though the eutectic phases with a higher Ni content are known to be the more ductile and weaker constituent of the microstructure [14] the higher wear resistance of this constituent within the coatings might be explained by two features. A first explanation is the higher strength of the austenitic phase as a consequence of supersaturation and a second the missing of the lamellar harder CrNi solid solution and, therefore, the absence of internal phase boundaries. Even though a higher number of phase or grain boundaries may lead to an increased amount of initial cracks, in some materials the same phases may also slow down crack propagation. This can take place by arresting cracks and shortening crack lengths between certain phases, as found in high-strength, brittle materials, or by deflecting cracks around phases [19]. Still, for the eutectic phase in the cast and heat treated Cr60Ni40-alloy, this seems not to be the case.

For the Cr-rich constituent the better wear behavior of the coatings can be attributed to the much finer needle-shaped precipitates compared to the cast and heat treated state. It has been found in other studies that grain refinement alone can lead to an improved wear resistance against cavitation erosion [12, 18]. However, the internal structure of these constituents is not fully understood yet, and proof of the different phases present as well as their mechanical properties still needs to be investigated. Further characteristics of this complex microstructure, e.g. possible precipitation hardening by ordered intermetallic phases might also contribute to the wear behavior.

5. Conclusions

Void free single and multiple overlapping coatings from Cr60Ni40 alloy were generated onto Nimonic 80A substrate by friction surfacing.

The coatings show a microstructure basically similar to the cast and heat treated state, with two main constituents, one with about 60 wt-% Cr and one with about the eutectic composition, as well as spherical non-metallic inclusions which are not affected by the process

While in the cast and heat treated state one constituent shows a lamellar eutectic consisting of an austenitic Ni-rich fcc and a Cr-rich bcc phase, within the coatings it depicts a supersaturated solid solution with an austenitic lattice.

The other main constituent containing 60 wt-% Cr is assumed to be a Cr-rich solid solution with needle-shaped Ni-rich precipitates of Widmannstätten type. These are much finer in the coatings than in the cast and heat treated state.

The coatings show a significantly better wear resistance against cavitation, with wear rates being about one third of the ones of the cast and heat treated material.

Improved wear resistance of the coatings is due to the refinement of the needle-shaped structure in the Cr-rich constituent and the absence of eutectic lamellae in the one with the eutectic composition. The latter leads to an increased strength by solid solution hardening and the absence of additional phase boundaries. This decreases the number of possible voids to be attacked during cavitation.

Acknowledgements

The authors wish to thank David Wiens, Robert Cichon, Stanislav Gorelkov and Birgit Gleising of the University of Duisburg-Essen for their efforts in cavitation testing and metallography.

References

[1] W. Herda, G. L. Swales, Neue Nickel-Chrom-Legierungen mit hoher Beständigkeit gegen Brennstoffaschenkorrosion, Werkstoffe und Korrosion, 19/8 (1968) 679-689.

[2] ASTM International, Standard Specification for Castings, Chromium-Nickel Alloy, ASTM 560/A 560 M, 1993.

[3] M.B. Vollaro, D.I. Potter, Phase formation in coevaporated Ni-Cr thin films, Thin Solid Films, 239 (1994) 37-46.

[4] A.R. Sethuraman, R.J. De Angelis, P.J. Reucroft, Diffraction studies on Ni-Co and Ni-Cr alloy thin films, Journal of Material Research, 6/4 (1991) 749-754.

[5] C. Sarbu, S.A. Rau, N. Popescu-Pogrion, M.I. Birjega, The Structure of Flash-Evaporated Cr-Ni (65:35) and Cr-Ni (50:50) Thin Films, Thin Solid Films, 28 (1975) 311-322.

[6] M.I. Birjega, M. Alexe, The influence of the argon pressure and substrate temperature on the structure of r.f.-sputtered CrNi(65:35), CrNi(50:50) and CrNi(20:80) thin films, Thin Solid Films, 275 (1996) 152-154.

[7] P. Nash, The Cr-Ni (Chromium-Nickel) System, Bulletin of Alloy Phase Diagrams, 7/5 (1986) 466-476.

[8] L. Kaufman, H. Nesor, Calculation of the Binary Phase Diagrams of Iron, Chromium, Nickel and Cobalt, Zeitschrift für Metallkunde, 64/4 (1973) 249-257.
[9] www.calphad.com/nickel-chromium.html, Computational Thermodynamics Inc., Carnegy, USA, 2006.
[10] J.Q. Li, T. Shinoda, Underwater friction surfacing, Surface Engineering 16/1 (2000) 31–35.
[11] H. Khalid Rafi, G.D. Janaki Ram, G. Phanikumar, K. Prasad Rao, Microstructural evolution during friction surfacing of tool steel H13, Materials and Design 32 (2011) 82-87.
[12] S. Hanke, A. Fischer, M. Beyer, J. dos Santos, J, Cavitation erosion of NiAl-bronze layers generated by friction surfacing, Wear, 273/1 (2011) 32-37.
[13] ASTM International, Standard Test Method for Cavitation Erosion Using Vibratory Apparatus, G 32-03, 2003.
[14] R. Kossowsky, Creep Behavior of Ni-Cr Lamellar Eutectic Alloy, Metallurgical Transactions, 1/6 (1970) 1909-1919.
[15] G.F. Sarzhan, V.I. Trefilov, S.A. Firstov, Study of the disintegration of a supersaturated solid solution on Chromium base in the system Cr-Ni, Fiz. metal. metalloved. 31/2 (1971) 294-298.
[16] X.M. Liu, Z.D. Zou, Y.H. Zhang, S.Y. Qu, X.H. Wang, Transferring mechanism of the coating rod in friction surfacing, Surface & Coatings Technology, 202 (2008) 1889-1894.
[17] G.M. Bedford, V.I. Vitanov, I.I. Voutchkov, On the thermo-mechanical events during friction surfacing of high speed steels, Surface and Coatings Technology, 141 (2001) 34-39.
[18] T. Kawazoe, A. Ura, M. Saito, S. Nishikido, Erosion characteristics of surface hardened Ni–Al bronze, Surface Engineering, 13/1 (1997) 37–40.
[19] A. Momber, R. Kovacevic, Fracture of brittle multiphase materials by high energy water jets, Journal of Materials Science 31 (1996) 1081-1085.